ARTICLE IN PRESS

Available online at www.sciencedirect.com

SCIENCE DIRECT®

Journal of Molecular Spectroscopy 233 (2005) 244–255

Journal of MOLECULAR SPECTROSCOPY

www.elsevier.com/locate/jms

Near infrared spectroscopy of NiF

M. Benomier [a], A. van Groenendael [a], B. Pinchemel [a,*], T. Hirao [b,1], P.F. Bernath [b]

[a] Laboratoire PhLAM, UMR CNRS 8523, Centre d'Etudes et de Recherches Lasers et Applications, Université de Lille I 59655 Villeneuve d'Ascq Cedex, France

[b] Department of Chemistry, University of Waterloo, Waterloo, Ont., Canada N2L 3G1

Received 17 May 2005; in revised form 27 June 2005

Abstract

Four new electronic transitions of NiF, recorded by high-resolution Fourier transform spectroscopy, have been located in the near infrared spectral region. The three new upper electronic states are labeled as $[12.5]^2\Delta_{5/2}$, $[9.9]\Omega = 1/2$ and $[6.3]^2\Pi_{3/2}$. In addition, the first excited state located at 251 cm^{-1} above the ground $X^2\Pi_{1/2}$ state has been revisited on the basis of the work carried out by Kopp and Hougen [Can. J. Phys. 45 (1967) 2581–2596], who showed that an $\Omega = 1/2$ state can be described either as a $^2\Sigma$ state or a $^2\Pi_{1/2}$ state. For NiF, both descriptions of this state have large fine-structure constants with $\gamma = -0.9599$ cm^{-1} for a $^2\Sigma$ description and $p = -0.7399$ cm^{-1} for a $^2\Pi_{1/2}$ description consist with a state of mixed character. If this low-lying state is considered to be a $[0.25]^2\Pi_{1/2}$ state rather than a $[0.25]^2\Sigma$ state (as proposed up to now), then the experimental pattern of the low-lying electronic states of NiF is similar to those of the related molecules NiH and NiCl.

Keywords: Nickel fluoride; High-resolution spectroscopy; Infrared electronic spectroscopy; Diatomic molecules; Fourier transform spectroscopy

1. Introduction

In a recent paper [1], three near infrared transitions of NiF have been studied leading to the identification of two new electronic states: a $^2\Pi_{3/2}$ state located at 11096.05 cm^{-1} and a $^2\Phi_{7/2}$ state located at 12008.92 cm^{-1} above the $X^2\Pi_{3/2}$ ground state. The presence of five close-lying spin–orbit components ($X^2\Pi_{3/2}$, $[0.25]^2\Sigma^+$, $[0.83]^2\Delta_{5/2}$, $[1.5]^2\Sigma^+$, and $[2.2]^2\Delta_{3/2}$) of three electronic states in the 0–2500 cm^{-1} energy range above the $X^2\Pi_{3/2}$ ground state leads to the observation of numerous electronic transitions. In this paper, we describe four new electronic transitions linking three new doublet electronic states of NiF: the $[6.3]\Omega = 3/2$ state located at 6311.18 cm^{-1}, the $[9.9]\Omega = 1/2$ state located at 9901.07 cm^{-1}, and the $[12.5]\Omega = 5/2$ state located at 12567.76 cm^{-1}. An extensive bibliography concerning the known transitions and the energy level diagram of NiF can be found in [1,2].

2. Experimental details

The experimental details have been described in [1]. The band located at 11737.7 cm^{-1} has been recorded using a silicon photodiode detector in exactly the same conditions as the bands previously published [1]. The bands located near 6300 and 10 000 cm^{-1} have been recorded with an InSb detector. In both cases, a CaF_2 beamsplitter has been used with a Bruker IFS 120 HR Fourier transform spectrometer. As for the previous experiments [1,2] all the experimental work was carried out at the University of Waterloo.

The molecular source consists of a 1.2 m long, 5 cm diameter alumina tube. A few grams of NiF_2 were

* Corresponding author. Fax: +33 3 20 43 40 84.
E-mail address: bernard.pinchemel@univ-lille1.fr (B. Pinchemel).
1 Present address: Institute for Astrophysics and Planetary Sciences, Ibaraki University, 2-1-1 Bunkyo, Mito, Ibaraki 310-8512, Japan.

0022-2852/$ - see front matter © 2005 Elsevier Ltd All rights reserved.
doi:10.1016/j.jms.2005.07.002

placed in the center of the tube and heated to 930 °C by a high temperature furnace. The pressure of the argon buffer gas was about 1000 Pa and a DC discharge (3000 V, 0.3 A) was struck between two stainless steel electrodes. An intense blue-white light was focused on the entrance aperture of the spectrometer with a lens.

3. The $[6.3]^2\Pi_{3/2} - X^2\Pi_{3/2}$ transition

This transition has the longest wavelength in our spectrum of NiF, which has been recorded down to 5400 cm^{-1}. The absence of a Q branch suggests that this transition has $\Delta\Omega = 0$. Two R heads are observed at 6330.896 and 6327.315 cm^{-1}. One observes that the R heads are relatively far from the origin of the band as compared to the other red and infrared transitions, which suggests that the rotational constants (B's) for the two states are nearly the same. Two P branches are also observed and more than 200 lines (Table 1) for the four branches have been identified. It was easy to determine that the only possible lower state (among the five low-lying spin–orbit components) of this transition is the $X^2\Pi_{3/2}$ ground state. Consistent with this assignment is the fact that the lambda-doubling splitting is proportional to J^3.

A localized perturbation was found in the R_{ff} and P_{ff} branches which has a maximum between the rotational levels $J' = 24.5$ and $J' = 25.5$ of the upper state. Despite the fact that the P_{ee} branch has been observed up to $J = 73.5$, no perturbation has been detected in the e levels of the upper state. The experimental lines have been fitted using a classical polynomial expression to account for the energy levels of both states:

$$T = T_v + B_v J(J+1) - D_v J^2(J+1)^2 \pm \tfrac{1}{2} p_J J(J+1)(J+1/2).$$

To break the strong correlation between the two lambda-doubling parameters, we included the microwave data published by Tanimoto et al. [3] in the fit. The derived parameters are listed in Table 2.

The value determined for the rotational constant of the upper state ($B'_0 = 0.379519$ cm^{-1}) is significantly different from any of the values observed for the nearby electronic states which have 0.361 $cm^{-1} < B_0 <$ 0.376 cm^{-1}. The value of B'_0 is rather close to most of the rotational parameters determined for the electronic states located between 18 000 cm^{-1} and 23 500 cm^{-1} (0.3792 $cm^{-1} < B_0 <$ 0.3796 cm^{-1}). The presence of a lambda-doubling splitting proportional to J^3 is consistent with the identification of this state as a $^2\Pi_{3/2}$ state. Nevertheless, a $^2\Pi_{3/2}$ state should be linked to the $[0.83]A^2\Delta_{5/2}$ state through an allowed transition at 5481 cm^{-1} which is not observed in our spectra. So there is no doubt that the upper state is a $\Omega = 3/2$ spin–orbit component, but the symmetry of this state is not firmly determined. There is also no trace of a transition occurring between the $[6.3]^2\Pi_{3/2}$ and the $[0.25]^2\Sigma^+$ state expected at 6060 cm^{-1}. Possible transitions connecting with the $[1.5]B^2\Sigma$ and the $[2.2]A^2\Delta_{3/2}$ states are out of the range of the recorded spectral region.

4. The $[12.5]\Omega = 5/2 - [0.83]A^2\Delta_{5/2}$ transition

The 11 400–11 800 cm^{-1} spectral region includes numerous blended bands. At 11 722 cm^{-1} is probably located the $[11.1]^2\Pi_{3/2}(v' = 1) - X^2\Pi_{3/2}(v'' = 0)$ transition. The band of this group at the high wavenumber end is a weak one with a head at 11743.4 cm^{-1}. This band does not exhibit any splitting of the lines, suggesting that the lower state of the transition is the $[0.83]A^2\Delta_{5/2}$ spin–orbit component of the $A^2\Delta_i$ state. The $[0.83]A^2\Delta_{5/2}$ spin–orbit component is the only one of the low-lying states for which no fine structure can be seen. With the absence of a Q branch, this band can be identified as a $[12.5]\Omega = 5/2 - [0.83]A^2\Delta_{5/2}$ transition. The fit of the 130 observed lines (Table 1) confirms the assumption about the nature of the lower state. The parameters derived from the fit are presented in Table 2. The upper state located at 12567.73 cm^{-1} is about 560 cm^{-1} above the $[12.0]^2\Phi_{7/2}$ state [1] but with the absence of the observation of the allowed $[12.5]^2\Phi_{5/2} - [2.2]A^2\Delta_{3/2}$ transition, the hypothesis of an upper $[12.5]^2\Phi_{5/2}$ state does not hold. In addition, the two rotational constants are too different ($B_0 = 0.36126$ cm^{-1} for the $[12.5]\Omega = 5/2$ state and $B_0 = 0.365925$ cm^{-1} for the $[12.0]^2\Phi_{7/2}$) state to be associated with two spin–orbit components of the same $^2\Phi_i$ state. On the other hand, the hypothesis of a $[12.5]^2\Delta_{5/2}$ state should lead to the observation of an allowed transition to the ground $X^2\Pi_{3/2}$ state at 12 567 cm^{-1}, but no band is observed in the experimental spectra at this location. No confusion can occur with the $v = 1$ vibrational level of the $[12.0]^2\Phi_{7/2}$ state because this level has been located at 12629.84 cm^{-1} [1]. In presence of such contradictions one cannot eliminate the possibility that the upper state of this transition could be, for example, a component of a quartet state.

5. The $[9.9]\Omega = 1/2 - [0.25]^2\Sigma^+$ and the $[9.9]\Omega = 1/2 - X^2\Pi_{3/2}$ transitions

In the visible spectral region it has been possible to identify transitions sharing the same upper state using the technique of laser-induced fluorescence, but such a method is difficult to use in the infrared. In some cases, it is possible to deduce the presence of a common upper state of two (or more) transitions when one observes that the bands are separated by an interval that corresponds to the known difference in energy levels of two

Table 1
Observed lines positions (in cm^{-1}) of the studied transitions of $^{58}Ni^{19}F$

J	P	R	J	P	R
$[12.5]\Omega = 5/2\ (v' = 0) - A[0.83]^2\Delta_{5/2}\ (v'' = 0)$					
3.5		11741.097	37.5	11671.985	11726.671
4.5		11741.580	38.5	11669.169	11725.281
5.5		11742.003	39.5	11666.303	11723.840
6.5	11732.272	11742.372	40.5	11663.391	11722.351
7.5	11731.136	11742.683	41.5	11660.415	11720.797
8.5	11729.940	11742.952	42.5	11657.399	11719.190
9.5	11728.703	11743.141	43.5	11654.312	11717.536
10.5	11727.413	11743.286	44.5	11651.183	11715.824
11.5	11726.063		45.5	11647.992	11714.065
12.5	11724.657		46.5	11644.760	11712.251
13.5	11723.203		47.5	11641.465	11710.367
14.5	11721.695	11743.362	48.5	11638.117	11708.440
15.5	11720.115	11743.229	49.5	11634.723	11706.459
16.5	11718.506	11743.046	50.5	11631.276	11704.420
17.5	11716.834	11742.820	51.5	11627.782	11702.324
18.5	11715.107	11742.530	52.5	11624.211	11700.177
19.5	11713.319	11742.193	53.5	11620.600	11697.974
20.5	11711.475	11741.782	54.5		11695.715
21.5	11709.588	11741.336	55.5	11613.217	11693.413
22.5	11707.641	11740.828	56.5	11609.448	11691.054
23.5	11705.644	11740.268	57.5	11605.623	11688.623
24.5	11703.587	11739.654	58.5	11601.745	11686.152
25.5	11701.481	11738.980	59.5	11597.815	11683.612
26.5	11699.321	11738.254	60.5	11593.837	11681.035
27.5	11697.105	11737.472	61.5	11589.797	11678.400
28.5	11694.834	11736.639	62.5	11585.715	11675.710
29.5	11692.510	11735.748	63.5	11581.558	11672.957
30.5	11690.130	11734.805	64.5	11577.379	11670.150
31.5	11687.702	11733.806	65.5	11573.125	11667.306
32.5	11685.213	11732.753	66.5	11568.833	11664.388
33.5	11682.673	11731.646	67.5	11564.478	11661.429
34.5	11680.077	11730.482	68.5		11658.422
35.5	11677.434	11729.269	69.5		11655.342
36.5	11674.739	11727.998	70.5		11652.210

J	P_{ee}	R_{ee}	P_{ff}	R_{ff}	Q_{ef}	Q_{fe}
$[9.9]\Omega = 1/2(v' = 0) - X^2\Pi_{3/2}\ (v'' = 0)$						
1.5					9903.004	
2.5					9903.929	9898.021
3.5					9904.836	9896.939
4.5				9898.992	9905.712	
5.5				9898.631	9906.568	9894.732
6.5		9914.023	9889.677	9898.240	9907.394	9893.593
7.5		9915.596	9887.781	9897.824	9908.207	9892.434
8.5		9917.124	9885.825	9897.386	9908.991	9891.251
9.5		9918.651	9883.863	9896.938	9909.748	9890.049
10.5			9881.854	9896.446	9910.492	9888.812
11.5	9901.601	9921.613	9879.855	9895.922	9911.193	9887.559
12.5	9901.549	9923.061	9877.820	9895.411	9911.880	9886.281
13.5	9901.468	9924.486	9875.760	9894.832	9912.540	9884.986
14.5	9901.371	9925.889	9873.677	9894.253	9913.177	9883.664
15.5	9901.244	9927.270	9871.564	9893.637	9913.790	9882.322
16.5	9901.108	9928.629	9869.437	9893.012	9914.379	9880.958
17.5	9900.938	9929.964	9867.271	9892.352	9914.943	9879.570
18.5	9900.755	9931.275	9865.086	9891.665	9915.485	9878.159
19.5	9900.554	9932.567	9862.881	9890.955	9916.000	9876.729
20.5	9900.325	9933.834	9860.647	9890.226	9916.488	9875.275
21.5	9900.066	9935.083	9858.394	9889.468	9916.952	9873.801
22.5	9899.794	9936.306	9856.112	9888.674	9917.392	9872.301
23.5	9899.504	9937.508	9853.802	9887.870	9917.810	9870.788
24.5	9899.181	9938.690	9851.475	9887.038	9918.201	9869.247

(continued on next page)

Table 1 (*continued*)

J	P_{ee}	R_{ee}	P_{ff}	R_{ff}	Q_{ef}	Q_{fe}
25.5	9898.840	9939.852	9849.115	9886.182	9918.567	9867.688
26.5	9898.490	9940.990	9846.748	9885.298	9918.909	9866.104
27.5	9898.113	9942.106	9844.343	9884.393	9919.225	9864.505
28.5	9897.713	9943.200	9841.921	9883.459	9919.517	9862.881
29.5	9897.293	9944.277	9839.462	9882.497	9919.788	9861.236
30.5	9896.856	9945.329	9836.987	9881.523	9920.030	9859.573
31.5	9896.391	9946.362	9834.490	9880.505	9920.242	9857.886
32.5	9895.923	9947.372	9831.962	9879.472	9920.439	9856.181
33.5	9895.411	9948.364	9829.415	9878.414	9920.605	9854.456
34.5	9894.900	9949.334	9826.839	9877.327	9920.749	9852.708
35.5	9894.362	9950.280	9824.228	9876.205	9920.860	9850.944
36.5	9893.805	9951.211	9821.619	9875.077	9920.960	9849.158
37.5	9893.227	9952.124	9818.972	9873.917	9921.034	9847.354
38.5	9892.635	9953.010	9816.299	9872.733		9845.530
39.5	9892.019	9953.880	9813.608	9871.525		9843.687
40.5	9891.384	9954.730	9810.886	9870.287		9841.823
41.5	9890.734	9955.563	9808.140	9869.024		9839.940
42.5	9890.049	9956.375	9805.373	9867.733		9838.045
43.5	9889.378	9957.166	9802.582	9866.419		9836.123
44.5	9888.674	9957.935	9799.766	9865.086	9920.809	9834.184
45.5	9887.945	9958.689	9796.922	9863.720	9920.672	9832.230
46.5	9887.206	9959.423	9794.056	9862.332	9920.522	9830.253
47.5	9886.448	9960.136	9791.165	9860.929	9920.336	9828.260
48.5	9885.667	9960.836	9788.256	9859.476	9920.131	9826.249
49.5	9884.876	9961.514	9785.316	9858.021	9919.899	9824.228
50.5	9884.071	9962.173	9782.353	9856.526	9919.649	9822.177
51.5	9883.238	9962.805	9779.370	9855.008	9919.363	9820.112
52.5	9882.394	9963.439	9776.360	9853.477	9919.051	9818.032
53.5	9881.523	9964.044	9773.319	9851.899	9918.724	9815.935
54.5	9880.647	9964.629	9770.267	9850.303	9918.376	9813.819
55.5	9879.758	9965.204	9767.187	9848.686	9918.003	9811.684
56.5	9878.842	9965.757	9764.080	9847.051	9917.591	9809.542
57.5	9877.924	9966.287	9760.947	9845.379	9917.158	9807.376
58.5	9876.980	9966.805	9757.798	9843.687	9916.707	9805.195
59.5	9876.025	9967.307	9754.616	9841.972	9916.230	9803.001
60.5	9875.043	9967.791	9751.421	9840.218	9915.725	9800.787
61.5	9874.078	9968.265	9748.195	9838.465	9915.199	9798.561
62.5	9873.059	9968.708	9744.952		9914.647	9796.315
63.5	9872.038	9969.145	9741.676		9914.073	9794.056
64.5	9870.996	9969.564	9738.383		9913.473	9791.779
65.5	9869.967	9969.965	9735.081		9912.848	9789.493
66.5	9868.898	9970.350	9731.719		9912.198	9787.188
67.5	9867.828		9728.354		9911.524	9784.865
68.5	9866.743		9724.977		9910.830	9782.537
69.5	9865.642				9910.096	9780.187
70.5					9909.372	9777.824
71.5	9863.404				9908.605	9775.446
72.5					9907.790	9773.062
73.5					9906.972	9770.668
74.5					9906.130	9768.245
75.5					9905.261	9765.802
76.5					9904.375	9763.366
77.5					9903.463	
78.5					9902.517	
$[9.9]\Omega = 1/2(v' = 0) - [0.25]^2\Sigma^+\ (v'' = 0)$						
1.5			9645.331			
2.5			9642.667			
3.5		9660.815	9639.949			
4.5		9663.293	9637.200			
5.5		9665.742	9634.448			
6.5		9668.172	9631.660		9649.369	9647.726
7.5		9670.564	9628.843		9649.283	9647.403

(*continued on next page*)

Table 1 (*continued*)

J	P_{ee}	R_{ee}	P_{ff}	R_{ff}	Q_{ef}	Q_{fe}
8.5	9657.456	9672.935	9625.988		9649.162	9647.047
9.5	9658.286	9675.274	9623.137		9649.010	9646.667
10.5	9659.086	9677.590	9620.233	9634.802	9648.837	9646.245
11.5	9659.860	9679.864	9617.312	9633.384	9648.637	9645.808
12.5	9660.609	9682.118	9614.349	9631.911	9648.415	9645.331
13.5	9661.333	9684.339	9611.374		9648.154	9644.837
14.5	9662.030	9686.536	9608.372	9628.952	9647.872	9644.315
15.5	9662.702	9688.703	9605.335		9647.556	9643.749
16.5	9663.355	9690.838	9602.278	9625.846	9647.228	9643.160
17.5		9692.945	9599.192	9624.250	9646.862	9642.547
18.5	9664.494	9695.020	9596.076		9646.465	9641.908
19.5	9665.081	9697.073	9592.938	9621.024	9646.054	9641.239
20.5	9665.579	9699.091	9589.776	9619.336	9645.609	9640.537
21.5	9666.048	9701.083	9586.581	9617.650	9645.134	9639.803
22.5	9666.535	9703.042	9583.362	9615.953	9644.641	9639.044
23.5	9666.959	9704.974	9580.119		9644.119	9638.242
24.5	9667.375	9706.876	9576.849	9612.401	9643.570	9637.447
25.5	9667.739	9708.749	9573.555		9642.996	9636.585
26.5	9668.089	9710.592	9570.231	9608.764	9642.395	9635.707
27.5	9668.429	9712.405	9566.882	9606.918	9641.770	9634.802
28.5	9668.701	9714.186	9563.512	9605.049	9641.115	9633.866
29.5	9668.976	9715.939	9560.111	9603.141	9640.434	9632.900
30.5	9669.188	9717.661	9556.684		9639.727	9631.910
31.5		9719.354	9553.238		9638.993	9630.870
32.5	9669.566	9721.017	9549.760	9597.281	9638.242	9629.834
33.5	9669.712	9722.652	9546.261	9595.262	9637.447	9628.742
34.5	9669.820	9724.255	9542.737		9636.647	9627.628
35.5	9669.905	9725.828	9539.186		9635.805	9626.486
36.5	9669.947	9727.367	9535.610		9634.952	9625.310
37.5	9669.978	9728.881	9532.012		9634.065	9624.107
38.5	9669.978	9730.359	9528.388		9633.156	9622.882
39.5	9669.947	9731.808	9524.740		9632.221	9621.616
40.5		9733.233	9521.067		9631.262	9620.316
41.5	9669.789	9734.620	9517.369		9630.274	9618.999
42.5	9669.661	9735.979	9513.645		9629.268	9617.650
43.5	9669.521	9737.307	9509.902		9628.236	9616.265
44.5	9669.326	9738.605	9506.132		9627.176	9614.848
45.5	9669.120	9739.873	9502.339		9626.093	9613.410
46.5	9668.901	9741.109	9498.521		9624.984	9611.926
47.5	9668.597	9742.314	9494.682		9623.851	9610.436
48.5		9743.487	9490.820		9622.695	9608.905
49.5		9744.631	9486.932		9621.515	9607.343
50.5		9745.744	9483.022		9620.316	9605.751
51.5		9746.824	9479.088		9619.083	9604.127
52.5		9747.876	9475.131		9617.831	9602.468
53.5		9748.896	9471.152		9616.555	9600.787
54.5		9749.883	9467.150		9615.262	9599.073
55.5		9750.839	9463.129		9613.935	9597.326
56.5		9751.771	9459.082		9612.589	9595.549
57.5		9752.657	9455.011		9611.224	9593.743
58.5		9753.523	9450.920		9609.830	9591.905
59.5		9754.351	9446.805		9608.416	9590.026
60.5		9755.158	9442.671		9606.978	9588.154
61.5		9755.925	9438.511		9605.514	9586.208
62.5		9756.659	9434.331		9604.035	9584.262
63.5		9757.363	9430.132		9602.528	9582.267
64.5		9758.042	9425.911		9601.003	9580.246
65.5		9758.682	9421.668		9599.453	9578.208
66.5		9759.291	9417.404		9597.880	9576.130
67.5		9759.872	9413.117		9596.287	9574.013
68.5		9760.417	9408.809		9594.668	9571.867
69.5		9760.944	9404.482		9593.029	9569.699
70.5		9761.419	9400.134		9591.365	9567.501
71.5		9761.870	9395.766		9589.695	9565.262

(*continued on next page*)

Table 1 (*continued*)

J	P_{ee}	R_{ee}	P_{ff}	R_{ff}	Q_{ef}	Q_{fe}
72.5		9762.297	9391.374		9587.985	9563.002
73.5		9762.681	9386.966		9586.262	9560.704
74.5		9763.041	9382.539		9584.523	9558.384
75.5		9763.367	9378.089		9582.752	9556.026
76.5		9763.664	9373.615		9580.958	9553.633
77.5		9763.917	9369.130		9579.158	
78.5			9364.617		9577.340	
79.5		9764.350	9360.093		9575.485	
80.5		9764.524	9355.548		9573.613	
81.5		9764.662	9350.980		9571.727	
82.5		9764.765	9346.396		9569.828	
83.5		9764.824	9341.799		9567.906	
84.5		9764.873	9337.173		9565.942	
85.5			9332.536		9563.984	
86.5			9327.871		9561.991	
87.5			9323.199			
88.5			9318.506			

J	P_{ee}	R_{ee}	P_{ff}	R_{ff}
$[6.6]^2\Pi_{3/2}(v'=0) - X^2\Pi_{3/2}(v''=0)$				
2.5	6309.215		6309.215	
3.5	6308.392	6314.468	6308.392	6314.468
4.5	6307.556	6315.150	6307.556	6315.150
5.5	6306.715	6315.820	6306.715	6315.820
6.5	6305.842	6316.469	6305.842	6316.469
7.5	6304.973	6317.108	6304.973	6317.108
8.5	6304.068	6317.716	6304.068	6317.716
9.5	6303.165	6318.338	6303.130	6318.307
10.5	6302.233	6318.931	6302.193	6318.886
11.5	6301.289	6319.502	6301.240	6319.446
12.5	6300.327	6320.062	6300.267	6319.989
13.5	6299.363	6320.600	6299.282	6320.519
14.5	6298.372	6321.137	6298.269	6321.028
15.5	6297.372	6321.650	6297.249	6321.517
16.5	6296.351	6322.144	6296.208	6321.993
17.5	6295.318	6322.628	6295.149	6322.447
18.5	6294.255	6323.096	6294.078	6322.883
19.5	6293.214	6323.544	6292.984	6323.315
20.5	6292.139	6323.990	6291.875	6323.728
21.5	6291.053	6324.417	6290.752	6324.138
22.5	6289.948	6324.821	6289.620	6324.567
23.5	6288.833	6325.229	6288.481	**6325.100**
24.5		6325.597	6287.364	**6324.650**
25.5	6286.557	6325.961	**6286.366**	6325.100
26.5	6285.403	6326.309	**6284.375**	6325.453
27.5	6284.233	6326.645	6283.252	6325.750
28.5	6283.045	6326.985	6282.073	6326.009
29.5	6281.854	6327.302	6280.821	6326.243
30.5	6280.642	6327.593	6279.541	6326.507
31.5	6279.421	6327.878	6278.232	6326.645
32.5	6278.188	6328.150	6276.899	6326.798
33.5	6276.938	6328.403	6275.549	6326.946
34.5	6275.680	6328.647	6274.169	6327.064
35.5	6274.409	6328.883	6272.775	6327.165
36.5	6273.126	6329.098	6271.357	6327.249
37.5	6271.830	6329.307	6269.919	6327.302
38.5	6270.525	6329.501	6268.464	
39.5	6269.205	6329.685	6266.988	
40.5	6267.876	6329.850	6265.488	
41.5	6266.536	6329.998	6263.969	
42.5	6265.183	6330.133	6262.440	
43.5	6263.819	6330.271	6260.872	6327.195

(*continued on next page*)

Table 1 (*continued*)

J	P_{ee}	R_{ee}	P_{ff}	R_{ff}		
44.5	6262.440	6330.387	6259.296	6327.098		
45.5	6261.059	6330.501	6257.693	6326.985		
46.5	6259.661	6330.582	6256.077	6326.852		
47.5	6258.262	6330.649	6254.436	6326.697		
48.5	6256.841	6330.726		6326.456		
49.5	6255.413		6251.084	6326.301		
50.5	6253.975		6249.381	6326.074		
51.5			6247.660	6325.822		
52.5	6251.084		6245.909	6325.542		
53.5			6244.140	6325.229		
54.5	6248.132		6242.346	6324.920		
55.5	6246.642		6240.527	6324.531		
56.5	6245.151		6238.682	6324.188		
57.5	6243.643		6236.823			
58.5	6242.132		6234.932			
59.5	6240.609					
60.5	6239.073					
61.5	6237.543					
62.5	6235.981					
63.5	6234.433					
64.5	6232.856					
65.5	6231.287					
66.5	6229.702					
67.5	6228.107					
68.5	6226.512					
69.5	6224.901					
70.5	6223.295					
71.5	6221.675					
72.5	6220.046					
73.5	6218.412					
J	P_{ee}	R_{ee}	P_{ff}	R_{ff}	Q_{ef}	Q_{fe}
$[9.9]\Omega = 1/2(v'=1) - X^2\Pi_{3/2}\ (v''=1)$						
4.5					9895.519	
5.5					9896.391	
6.5					9897.223	
7.5				9887.638	9898.022	9882.279
8.5				9887.173	9898.812	9881.090
9.5			9873.800	9886.754	9899.590	9879.900
10.5			9871.813	9886.249	9900.325	9878.685
11.5			9869.803	9885.729	9901.061	9877.454
12.5			9867.800	9885.194	9901.755	9876.204
13.5	9891.465		9865.746	9884.634	9902.426	9874.902
14.5	9891.384		9863.683	9884.071	9903.086	9873.603
15.5	9891.287		9861.597	9883.459	9903.707	9872.300
16.5	9891.165	9918.493	9859.476	9882.856	9904.309	9870.935
17.5	9891.018	9919.822	9857.350	9882.208	9904.887	9869.572
18.5	9890.865	9921.145	9855.201	9881.524	9905.441	9868.185
19.5	9890.685	9922.460	9853.029	9880.849	9905.974	9866.778
20.5	9890.482	9923.748	9850.807	9880.141	9906.486	9865.345
21.5	9890.265	9925.012	9848.581	9879.394	9906.972	9863.898
22.5	9890.049	9926.257	9846.334	9878.622	9907.428	9862.440
23.5	9889.760	9927.485	9844.064	9877.820	9907.870	9860.949
24.5	9889.468	9928.682	9841.761	9876.980	9908.283	
25.5	9889.183	9929.868		9876.205	9908.671	
26.5	9888.867	9931.040			9909.035	
27.5	9888.526	9932.176			9909.372	
28.5	9888.174	9933.298			9909.694	
29.5	9887.782	9934.400			9909.985	
30.5	9887.395	9935.487			9910.254	9849.933
31.5	9886.980	9936.551			9910.492	9848.315
32.5	9886.545	9937.599			9910.718	9846.642
33.5	9886.094	9938.622			9910.909	9844.965

(*continued on next page*)

Table 1 (*continued*)

J	P_{ee}	R_{ee}	P_{ff}	R_{ff}	Q_{ef}	Q_{fe}
34.5	9885.635	9939.628			9911.154	9843.260
35.5	9885.132	9940.613			9911.351	9841.547
36.5	9884.634	9941.584			9911.449	9839.808
37.5	9884.108	9942.531			9911.524	9838.046
38.5	9883.565	9943.463			9911.581	9836.279
39.5	9883.009	9944.380				9834.489
40.5	9882.428	9945.283				9832.683
41.5	9881.854	9946.149				9830.855
42.5	9881.227	9947.005				9829.010
43.5	9880.603	9947.858				9827.150
44.5	9879.965	9948.658				9825.273
45.5	9879.299	9949.498				9823.380
46.5	9878.623	9950.279				9821.472
47.5	9877.925	9951.040				9819.546
48.5	9877.221	9951.792				9817.598
49.5	9876.498					9815.639
50.5	9875.761					9813.660
51.5	9875.003				9910.492	9811.685
52.5	9874.224				9910.254	9809.667
53.5	9873.448				9909.927	9807.637
54.5	9872.645				9909.642	9805.604
55.5	9871.813				9909.299	9803.545
56.5	9870.996				9908.992	9801.478
57.5	9870.154				9908.587	9799.393
58.5	9869.283				9908.207	9797.299
59.5	9868.419				9907.790	9795.182
60.5	9867.509				9907.305	9793.064
61.5	9866.633				9906.845	9790.916
62.5	9865.698				9906.359	9788.759
63.5	9864.789				9905.860	9786.590
64.5	9863.839				9905.329	9784.417
65.5	9862.881				9904.781	9782.212
66.5	9861.911				9904.207	9780.000
67.5	9860.949				9903.610	9777.786
68.5	9859.934				9903.004	9775.548
69.5	9858.943				9902.387	9773.320
70.5	9857.928				9901.681	9771.033
71.5						9768.762
72.5						
73.5						9764.174
74.5					9898.750	9761.869
75.5					9897.935	
76.5					9897.122	
77.5					9896.348	

Bold face, maximum of the perturbation.

of the low-lying spin–orbit components of the X, A, and B states. This methods works very well when the bands are analyzed and their origins are known, but care must be used when only the band head positions are available. Two intense transitions in the 9500–10 000 cm^{-1} spectral range are well developed and spaced by about 250 cm^{-1}, which is the energy gap between the $X^2\Pi_{3/2}$ and the $[0.25]^2\Sigma^+$ states. This hypothesis was confirmed by a rough calculation of the $\Delta B = B' - B''$ values for the two transitions that showed that if the upper state was considered to be the same for the two transitions then the difference between the B_0 values for the two lower states was in good agreement with the expected value $(B_0([0.25]^2\Sigma^+) - B_0(X^2\Pi_{3/2}) = 0.0022\ \text{cm}^{-1})$ [2]. Although the two bands are partially overlapped, they both seemed to have a large fine structure. This is not surprising for the transition located at 9650 cm^{-1} because its lower state is the well known $[0.25]^2\Sigma^+$ state for which a large fine structure is observed [2,3]. For the other transition at 9900 cm^{-1} connected to the $X^2\Pi_{3/2}$ ground state, the unusual pattern of the lines indicated that the upper state was also affected by a large fine-structure splitting.

The analysis of the two transitions was made simultaneously because at each step it was necessary to confirm the assignment of a branch by the observation of a connected branch in the other transition. Most of the analysis has been based on combination differences and on

Table 2
Molecular constants (in cm^{-1}) for the electronic states involved in the observed transitions of $^{58}Ni^{19}F$ (all uncertainties are 1σ)

	$[12.5]\Omega = 5/2$	$[9.9]\Omega = 1/2$		$[6.3]\Omega = 3/2$	$[0.83]A^2\Delta_{5/2}$	$[0.25]^2\Sigma^+$ [c]	$X^2\Pi_{3/2}$	
	$v = 0$	$v = 0$	$v = 1$	$v = 0$	$v = 0$	$v = 0$	$v = 0$	$v = 1$
T_v	12567.7648(11)	9901.0740(10)	[a]	6311.1769(10)	829.4761[b]	251.2588(10)	0	[a]
B_v	0.361260(30)	0.3759948(12)	0.372671(57)	0.3795195(15)	0.388529(30)	0.39001397(50)	0.38781554(42)	0.383924(56)
$D_v \times 10^7$	5.199(40)	5.2266(82)	4.30(15)	6.092(19)	5.385(40)	5.5201(84)	6.1061(60)	5.17(15)
$H_v \times 10^{12}$		−1.059(55)				−1.201(57)		
p		1.972841(21)	1.97108(15)					
$p_J \times 10^5$		−0.03324(57)	−0.0290(66)	1.2222(48)			−2.3486(42)	−2.582(45)
γ						−0.959917(27)		
$\gamma_D \times 10^5$						1.8166(22)		
$\gamma_H \times 10^9$						0.0904(30)		

[a] $[9.9]\Omega = 1/2 - X^2\Pi_{3/2}$: $\nu_{1-1} = 9890.8635(23)$.
[b] From Ref. [2].
[c] See Section 6 and Table 3.

the known term values of the two lower electronic states [2,3]. The main problem was to determine the accurate position of the origins of the branches. We arbitrarily decided to assign the upper state as a $^2\Pi_{1/2}$ spin component. By chance, the P_{ee} branch of the $[9.9]\Omega = 1/2(v = 0) - X^2\Pi_{3/2}(v = 0)$ transition has the appearance of a Q branch (i.e., the origin of the P_{ee} branch is very close to the band head) so the origin of this transition was located at 9901 cm^{-1}, which turned out to be nearly correct (actual value is 9901.07 cm^{-1}). As a consequence the origin of the $[9.9]\Omega = 1/2(v = 0) - [0.25]^2\Sigma^+ (v = 0)$ transition was set at 9650 cm^{-1}. In such complicated spectra, in which no ‘‘textbook’’ pattern of lines is of any help, one cannot expect to ascertain directly the assignment of a branch by inspection. The knowledge of the term values for the two lower states, however, allowed us to build a coherent set of assignments for the two transitions. Six branches are observed for each transition and there are a total of about 780 lines. The two transitions have been fitted simultaneously and the microwave data collected by Tanimoto et al. [3] for the two lower states have been included in the fit.

Despite the goodness of the fit, it was important to check on the correctness of our description of the bands. In particular, the identification of the extra heads present near the $[9.9]\Omega = 1/2(v = 0) - X^2\Pi_{3/2}(v = 0)$ transition had to be carried out. About 250 lines have been collected, and they belong to the six branches of the $v' = 1 - v'' = 1$ band of the same transition. The analysis of this band is interesting for two reasons. First, it allows us to confirm the analysis of the $[9.9]\Omega = 1/2 - X^2\Pi_{3/2}$ transition, because without any constraints on the parameters, the derived constants (Table 2) are in good agreement with those derived for the $v' = 0 - v'' = 0$ band, despite the absence of information provided by microwave data. In addition, we note that it is the first time that rotational constants for the $v = 1$ level of the ground state have been determined. The most striking observation has been the very large value obtained for the fine-structure parameter in the upper state, $p = 1.9728$ cm^{-1} for the $v = 0$ vibrational level (and $p = 1.9711$ cm^{-1} for the $v = 1$ level) which explains the unusual pattern of the branches in the two transitions.

6. The $[0.25]^2\Sigma^+$ state

About 35 electronic transitions of NiF are observed in the visible and infrared spectral regions and most of them have been analyzed. As noted in Section 1, this large number of transitions is caused by the presence of three low-lying doublet electronic states in the first 2500 cm^{-1} of the energy level diagram (Fig. 1). Any $^2\Sigma$, $^2\Pi$, $^2\Delta$, and $^2\Phi$ excited state can find one or more

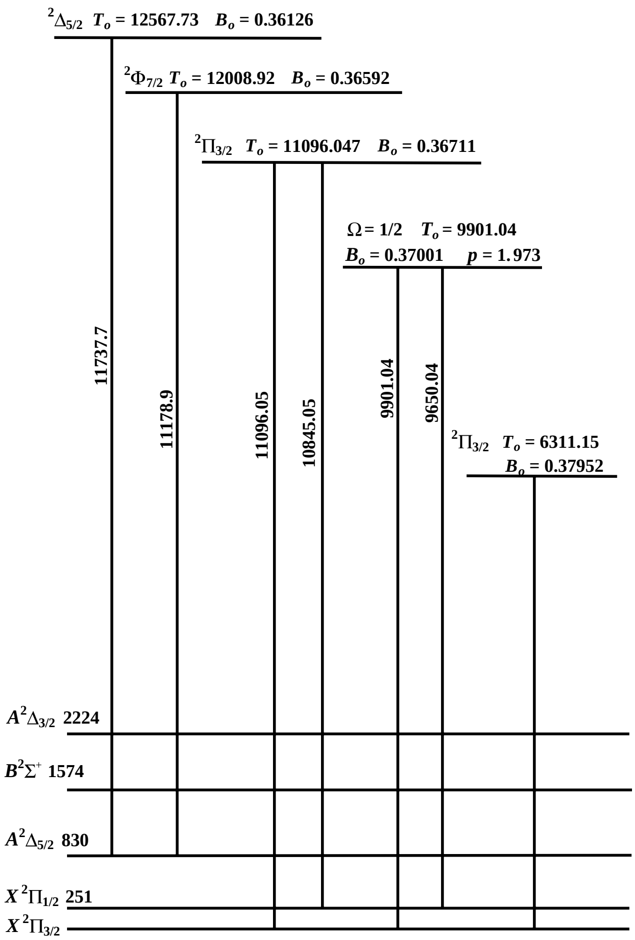

Fig. 1. Energy level diagram of the low-lying states of NiF, all the data are in cm^{-1}. The $[12.0]^2\Phi_{7/2}$ and $[11.0]^2\Pi_{3/2}$ states have been studied in [1]. In previous papers, the $[0.25]X^2\Pi_{1/2}$ state was labeled as $[0.25]^2\Sigma^+$.

low-lying partners to lead to one or more electronic transitions. Because of state mixing, forbidden transitions are also frequently observed in the spectrum of NiF.

The $A^2\Delta_i$ state is made of two spin–orbit components separated by about 1400 cm^{-1} and this value is almost equal to $2\xi = 1206\ cm^{-1}$ [4], where ξ is the spin–orbit coefficient of the ground $[3d^9]^2D$ electronic state of Ni^+ ion. This is expected if one assumes that the Ni^+F^- molecular orbitals and Ni^+ atomic orbitals are correlated in an ionic molecule [5]. The $X^2\Pi_{3/2}$ and the $[0.25]^2\Sigma^+$ states have been the subject of numerous papers including pure rotational analyses in the microwave spectral range [3]. The ground state is firmly identified as the $X^2\Pi_{3/2}$ spin–orbit component of a $^2\Pi_i$ state, but up to now the $X^2\Pi_{1/2}$ spin–orbit component has never been observed, despite numerous transitions which are possible. An extra state located at 251.25 cm^{-1} has been labeled as a $[0.25]^2\Sigma^+$ state based on dispersed laser-induced fluorescence [6]. A large fine-structure constant was observed ($\gamma = -0.96\ cm^{-1}$), and this value was confirmed by the analysis of the pure rotational spectrum [3]. In this work, Tanimoto et al. adopted the symmetry previously suggested for this state [6]. It is tempting to suggest that the $[0.25]^2\Sigma^+$ state is in fact the second spin–orbit component of the ground state, despite the fact that the interval between the two components (251 cm^{-1}) is not equal to the atomic spin–orbit coefficient ξ (=603 cm^{-1}) of Ni^+ as expected from metal-centered molecular orbitals.

Some time ago Kopp and Hougen [7] showed that any $\Sigma_{1/2}$ state could be fitted as a $\Pi_{1/2}$ state or vice versa. In the case of doublet states, for example, the fine-structure parameters (γ for the $^2\Sigma$ state and p for the $^2\Pi_{1/2}$ state) are linked by the relationship:

$$\gamma - p = 2B. \quad (1)$$

These two alternate descriptions of a state do not change the values of the rotational constants or the e/f labeling of the fine structure. In most of the cases it is obvious that the adopted description (Σ or $\Pi_{1/2}$) is the one which leads to the smallest value of the fine-structure parameter (γ or p). This choice is more difficult if the fine-structure parameter derived for an electronic state is larger than the rotational constant as it is for the $[0.25]^2\Sigma^+$ state of NiF ($\gamma = -0.96\ cm^{-1}$ and $B = 0.3900\ cm^{-1}$).

The 375 experimental lines of the $[9.9]\Omega = 1/2 - [0.25]^2\Sigma^+$ transition (studied in Section 5) and the nine microwave data available for the lower state have been fitted with the lower state as either a $^2\Sigma^+$ state or as a $^2\Pi_{1/2}$ state. The quality of the two fits is equivalent and the rotational constants B and D are not affected by the two different descriptions of the lower state (Table 3). The values derived for the third order H parameters are not in good agreement, but their uncertainties are too large to allow us to trust in the significance of these parameters. The fine-structure parameters of the upper $[9.9]\Omega = 1/2$ state are not affected by the description of the lower state. As expected, for the lower $[0.25]^2\Sigma^+$ state, the fine-structure parameters γ and p fulfill Eq. (1) given by Kopp and Hougen [6]: $(-0.959896\ cm^{-1}) - (-1.739887\ cm^{-1}) = 2 \times 0.389995\ cm^{-1}$.In the same way, we observe that the second order parameters γ_D and p_J are linked to D through the relationship, $\gamma_D - p_J = -4D$.

From a discussion with Tanimoto [8], it seems to be possible to fit the microwave data alone by adopting a different choice for the way the e and f fine-structure levels are associated together. For the hypothesis of a $^2\Pi_{1/2}$ state, the fit of the lines is very good, the B and D parameters are not affected, but the values of the fine-structure parameters were found equal to $p = -0.17967\ cm^{-1}$ and $p_J = 0.1568 \times 10^{-4}\ cm^{-1}$. This result was very puzzling because such a value of p made the state lying at 251 cm^{-1} an "ordinary" $^2\Pi_{1/2}$ state (but with a fairly large second order p_J parameter). In

Table 3
The two possible descriptions of the electronic state located at 251 cm^{-1} above the ground state

	Fitted as $[9.9]\Omega = 1/2 - [0.25]^2\Pi_{1/2}$		Fitted as $[9.9]\Omega = 1/2 - [0.25]^2\Sigma^+$	
	$[9.9]\Omega = 1/2$	$[0.25]^2\Pi_{1/2}$	$[9.9]\Omega = 1/2$	$[0.25]^2\Sigma^+$
T_v	9901.0740[a]	251.8369(74)	9901.0740[a]	251.2592(75)
B_v	0.3759985(16)	0.38999737(86)	0.3759969(16)	0.39001537(85)
$D_v \times 10^7$	5.289(20)	5.579(18)	5.264(20)	5.556(19)
$H_v \times 10^{12}$	0.31(10)	0.122(82)	0.05(10)	−0.103(62)
p	1.972913(32)	−1.739887(26)	1.972901(32)	
$p_J \times 10^5$	−0.0362(10)	2.0334(22)	−0.0359(10)	
$p_H \times 10^9$		0.1010(29)		
γ				−0.959896(27)
$\gamma_D \times 10^5$				1.8124(27)
$\gamma_H \times 10^9$				0.0993(29)

[a] Fixed value.

the two cases the fine-structure parameters are linked together by the relationship: $(p = -0.179673\ cm^{-1}) - (p = -1.739887\ cm^{-1}) = 4 \times (B = 0.390053\ cm^{-1})$. An equivalent relationship is observed between the second order parameters p_J, the difference of which is equal to $8 \times D$ [9]. The choice between the two $^2\Pi_{1/2}$ options was not clear.

To choose between the two possibilities, we decided to study a transition linking the [0.25] state to an upper state in which no fine structure is observed, i.e., the $[22.9]^2\Pi_{3/2} - [0.25]\Omega = 1/2$ transition [6]. A Fortrat diagram was constructed for the transition on the basis of the calculated term values for the lower state in the two cases ($p = -0.179673$ and $-1.739887\ cm^{-1}$). The constants for the upper $[22.9]^2\Pi_{3/2}$ state were those published in [2]. It turns out that only the energy level diagram associated with the constant $p = -1.739887\ cm^{-1}$ agreed with the experimental spectrum and that the diagram associated with the small value of $p = -0.179673\ cm^{-1}$ is not correct. It is obvious that on the basis of the term values of the lower state other choices of p are theoretically possible, and they are linked together by the relationship $\Delta p = 4B$. One can deduce that when the fine structure of an electronic state is larger than the rotational structure itself, then the determination of the fine-structure parameters must be confirmed by the analysis of an electronic transition between the state of interest and another already known state, and that pure rotational spectra, despite their very high resolution, are not sufficient to ascertain the fine-structure pattern. Surprisingly, pure rotational spectroscopy alone is ambiguous.

Table 4
Summary of the known electronic states of NiF

State	T_0 (cm)$^{-1}$	Vibration (cm^{-1})		Rotation (cm^{-1})		Equilibrium distance (Å)	
		ω_e	$\Delta G_{1/2}$	B_e	B_0	r_e	r_0
		[10]	Experimental				
$[23.5]^2\Pi_{1/2}$	23498.37	658.5	651		0.379425		1.76223
$[22.9]^2\Pi_{3/2}$	22955.19	665.06	656		0.379184		1.76279
$[20.4]\Omega = 3/2$	20405.71				0.37864		1.76406
$[20.3]^2\Pi_{1/2}$ [10]	20281.96	631.14			0.3844		1.751
$[20.1]^2\Pi_{1/2}$	20106.294				0.384863		1.74974
$[19.9]\Omega = 5/2$	19983.33	663.35	655	0.380966	0.379542	1.75866	1.76196
$[19.7]\Omega = 3/2$	19718.97				0.379601		1.76182
$[18.1]^2\Delta_{5/2}$	18107.37	661.62	656	0.380632	0.379187	1.75922	1.76278
$[12.5]\Omega = 5/2$	12567.76				0.361260		1.80599
$[12.0]^2\Phi_{7/2}$	12008.92		621	0.367292	0.365925	1.79110	1.79444
$[11.1]^2\Pi_{3/2}$	11096.05		619		0.367113		1.79154
$[9.9]\Omega = 1/2$	9901.07		634	0.377657	0.375995	1.76635	1.77025
$[6.3]\Omega = 3/2$	6311.18		621	0.38082	0.379519	1.77383	1.76201
$[2.2]A^2\Delta_{3/2}$	2223.57		653	0.390086	0.388427	1.73798	1.74169
$[1.5]B^2\Sigma^+$	1574.02		648	0.38771	0.38596	1.74330	1.74724
$[0.83]A^2\Delta_{5/2}$	829.48		653	0.390172	0.388529	1.73779	1.74146
$[0.25]^2\Sigma^+$	251.26		607		0.390014		1.73814
$X^2\Pi_{3/2}$	0		644	0.38976	0.387815	1.73871	1.74306

7. Conclusion

Three new spin components of excited states of NiF have been found. As usually observed in the spectrum of NiF, the symmetries of these states are not easily determined, because the selection rules are not strictly observed and generally only the value of Ω can be trusted. For example, the $\Omega = 5/2$ state located at $12567.7\ \mathrm{cm}^{-1}$ cannot be firmly identified as a component of a $^2\Delta$ or of a $^2\Phi$ state. The $[9.9]\Omega = 1/2$ state is even more difficult to label. As for the state lying at $251\ \mathrm{cm}^{-1}$ (section 6), it is possible to describe this state as a $^2\Pi_{1/2}$ state or as a $^2\Sigma^+$ state, and in both cases the fine-structure parameter is large ($p = 1.973\ \mathrm{cm}^{-1}$ for a $^2\Pi_{1/2}$ state or $\gamma = 2.713\ \mathrm{cm}^{-1}$ for a $^2\Sigma^+$ state). Clearly such large values are only consistent with a substantial mixing of the electronic character.

In Table 4 are summarized all the electronic and rovibrational constants which have been collected for the known electronic states of NiF. The electronic states located in the 6000–13 000 cm^{-1} region of the energy level diagram have rotational constants spread out over a relatively large range of values: $\Delta B = 0.0182\ \mathrm{cm}^{-1}$, while $\Delta B = 0.0040\ \mathrm{cm}^{-1}$ for the group of three lowest states, $X^2\Pi_i$, $A^2\Delta_i$, and $B^2\Sigma^+$, and $\Delta B = 0.0062\ \mathrm{cm}^{-1}$ for the group of excited states located between 18 000 and 23 500 cm^{-1}. As a consequence, it is difficult to identify the spin–orbit components for a given electronic state on the basis of a comparison of the rotational constants.

The low-lying states of NiF have been known for a long time and they can be compared to those of the related NiH [11] and NiCl [12] molecules. Recently, the NiCN molecule was also detected [13] and the low-lying states are similar. In the case of NiH and NiCl, the three low-lying states $^2\Pi_i$, $^2\Delta_i$, and $^2\Sigma^+$ have been identified but the energy order of the states is different depending on the molecule. In [13], Figs. 16 and 17 display energy level diagrams in which the relative positions of the low-lying electronic states of the four molecules of interest are compared. Up to now in the case of NiCN the $^2\Sigma^+$ and the $^2\Pi_{1/2}$ states have not been identified. Based on these comparisons, it was puzzling to observe for NiF in the first $2500\ \mathrm{cm}^{-1}$ above the ground state, the presence of two $^2\Sigma$ states and the absence of a $^2\Pi_{1/2}$ spin–orbit component associated with the well known ground $X^2\Pi_{3/2}$ state. Semi-empirical calculations based on ligand field theory [5] showed that such a situation disagreed with theoretical predictions. In the present paper we point out the fact that the $[0.25]X^2\Pi_{1/2}$ spin component is now identified, although there is a rather large difference between the rotational constants of the two spin–orbit components (Table 2). One can expect that ab initio calculations in progress [14] will soon provide more insight into the electronic structure of nickel monohalides.

References

[1] B. Pinchemel, T. Hirao, P.F. Bernath, J. Mol. Spectrosc. 215 (2002) 262–268.
[2] Y. Krouti, T. Hirao, C. Dufour, A. Boulezhar, B. Pinchemel, P.F. Bernath, J. Mol. Spectrosc. 214 (2002) 152–174.
[3] M. Tanimoto, T. Sakamaki, T. Okabayashi, J. Mol. Spectrosc. 207 (2001) 66–69.
[4] C.E. Moore, Atomic Energy Levels, vol. II, NBS, 1952.
[5] P. Carette, C. Dufour, B. Pinchemel, J. Mol. Spectrosc. 161 (1993) 323–335.
[6] C. Dufour, B. Pinchemel, J. Mol. Spectrosc. 173 (1995) 70–78.
[7] I. Koop, J.T. Hougen, Can. J. Phys. 45 (1967) 2581–2596.
[8] M. Tanimoto, private communication, 2003.
[9] M. Benomier, DEA report, University of Lille I, 2003.
[10] J. Jin, Q. Ran, X. Yang, Y. Chen, C. Chen, J. Phys. Chem. A 105 (2001) 11177–11182.
[11] J.A. Gray, M. Li, T. Nelis, R.W. Field, J. Chem. Phys. 95 (1991) 7164–7178.
[12] Y. Krouti, A. Poclet, T. Hirao, B. Pinchemel, P.F. Bernath, J. Mol. Spectrosc. 210 (2001) 41–50.
[13] C.T. Kingston, A.J. Merer, T.D. Varberg, J. Mol. Spectrosc. 215 (1995) 106–127.
[14] N. Rinskop, J. Liévin, private communication, 2005.